RESEARCH ARTICLE

Macromolecular Materials and Engineering
Open Access
www.mame-journal.de

Interaction Parameters of Some Polymers Used in Nuclear Power Plants with Ionizing Radiation, Produced Secondary Radiations and Radiation Damages

Ferdi Akman and Hasan Oğul*

The primary interactions of polypropylene (PP), poly(vinyl acetate) (PVA), ethylene-vinyl acetate (EVA), polyvinyl chloride (PVC), polychloroprene (CR) and polyurethane (PUR) polymers preferred in the nuclear industry with gamma and neutron radiations, secondary radiations formed after neutron interactions and damages given to polymers by these ionizing radiations are investigated. The gamma interaction parameters Were determined in the photon energy range of 0.03-20 MeV using WinXCOM, GEANT4 and FLUKA methods. Also, energy absorption and exposure buildup factors and Kerma parameters are calculated at different photon energies. To investigate the interactions of the studied polymers with neutron, the effective removal cross-section for fast neutrons with theoretical and the partial neutron rates passing through the studied polymer at 4.5 MeV, 100 eV and 0.025 eV energies are determined with simulation codes. The numbers of secondary gamma-rays and neutrons Were obtained with GEANT4. The Total Ionizing Dose and Displacements per Atom parameters are studied with the help of FLUKA simulation. It is observed that the interaction of PVC polymer with gamma radiation and PP polymer with neutron particles is higher than the others. The secondary radiation from PVC and CR is less. The PP, PVA, and EVA exhibit superior resistance to radiation damage.

1. Introduction

Since polymers have many uses in textile, health, building materials, and automotive industries, they have been the subject of research in many articles, books, or projects. It is frequently used in the textile industry to produce polyester or polyamide synthetic yarn. In the health sector, it is preferred in many areas such as prosthesis and orthosis production, stents, artificial skin production, surgical sutures, and drug delivery systems. In building materials, due to its properties such as lightness, durability, and ability to be shaped as desired, it has many areas such as floor covering, sealing material, use as a pipe in water installations, and use as an adhesive material. In the automotive industry, it is also preferred in seats, upholstery, electrical systems, fuel systems, and external parts. Apart from these, another important area of use of polymers is the nuclear industry, especially in nuclear power plants. Polymers are mostly preferred in this field in electrical insulation materials, waste containers, pipes, and sealing materials.[1] In other areas of the nuclear industry, polymers have applications in radioactive waste management, superabsorbent, and decontamination of nuclear agents. In such environments, where high-energy photons and neutrons are present, the interaction of polymers with ionizing radiation needs to be investigated. The primary reason for this requirement is that secondary radiations generated by polymers interacting with photons and neutrons will have adverse effects on living beings and electronic devices or signals. Apart from this, radiation damage to polymers used in the nuclear industry will impact their basic mechanisms such as fragmentation and cross-linking of macromolecular chains.[2] Even very small amounts of ionizing radiation can cause a change in the physical or mechanical characteristics of a polymer. Depending on the chemical structure of the polymer, the disruption of even a few cross-links in the molecule can cause significant changes in its strength.[3] There are many studies in the literature investigating the negative effects of radiation on polymers.[4–10] Apart from this, there are also studies on the usability of polymers in ionizing radiation shielding.[11–29] Because polymers contain elements with low atomic numbers, they may be particularly promising for neutron radiation shielding. In gamma radiation shielding, studies

F. Akman
Department of Property protection and Security
Program of Occupational Health and Safety
Vocational School of Social Sciences
Bingöl University
Bingöl 12000, Türkiye
E-mail: fakman@bingol.edu.tr
H. Oğul
Department of Nuclear Engineering
Faculty of Engineering and Architecture
Sinop University
Sinop 57000, Türkiye

The ORCID identification number(s) for the author(s) of this article can be found under https://doi.org/10.1002/mame.202400326

DOI: 10.1002/mame.202400326

are generally carried out on composites produced with polymers and materials with high atomic numbers and densities.[30–36] Elmahroug et al. determined the neutron and gamma radiation shielding capacities for some different types of polymer resins and reported that the coded 250WD resin would be better used in this area.[22] Kaçal et al. investigated the gamma radiation shielding properties experimentally and theoretically for polyamide, polyacrylonitrile, polyvinylidene chloride, polyaniline, polyethylene terephthalate, polyphenylene sulfide, polypyrrole and polytetrafluoroethylene polymers in the energy range of 81 to 1333 keV and also determined the neutron shielding capabilities of these polymers theoretically. They noted that the gamma and neutron radiation shielding properties of polytetrafluoroethylene and polyamide polymers were superior to the others, respectively.[24] While Alabsy et al. studied the gamma radiation shielding and exposure buildup factors of polymethylpentene, polybutylene terephthalate, polyoxymethylene, polyvinylidene fluoride, and polychlorotrifluoroethylene polymers using the GEANT4 simulation code,[26] Sayyed et al. studied the gamma and neutron radiation shielding characteristics of some smart polymers.[27]

In the presented study, the interaction parameters of PP, PVA, EVA, PVC, CR and PUR polymers, which are frequently used in the nuclear industry, with ionizing radiation were investigated. While PP, PVA, and EVA are preferred in cables, pipes, gaskets, and absorbent papers, PVC, CR, and PUR are preferred in cables, gloves, and glove box handles in nuclear power plants.[37] The reasons why polymers are preferred in this field include some of their properties such as low cost, lightness, high corrosion resistance, and low electrical conductivity compared to metals and other materials. In order to investigate the interactions of these polymers, which are used in important areas in the nuclear industry, with gamma radiation, mass (μ/ρ), and linear (μ) attenuation coefficients, half (HVL) and tenth (TVL) value layers, mean free path (MFP), effective atomic number (Z_{eff}), energy absorption (EABF) and exposure buildup (EBF) factors and kinetic energy released in material (Kerma) relative to X (X = air, water, ordinary concrete and lead glass) parameters were determined. To investigate the interaction of these polymers with neutrons, effective removal cross-section for fast neutrons (Σ_R) and relative neutron transmission ratios for fast (4.5 MeV), slow (100 eV), and thermal neutrons (0.025 eV) characteristics were determined. The number and average energy of secondary radiation species formed by these polymers at thermal, slow, and fast neutron energies were obtained. Finally, the total ionizing dose (TID) and displacement per atom (DPA) parameters were determined and radiation damage on the polymers was investigated in the long term.

2. Experimental Section

2.1. Theoretical Calculation Processes

The single-chain forms of PP, PVA, EVA, PVC, CR, and PUR polymers frequently used in nuclear power plants are C_3H_6, $C_4H_6O_2$, $C_6H_{10}O_2$, C_2H_3Cl, C_4H_5Cl, and $C_3H_8N_2O$, respectively. These polymers have densities of 0.855, 1.19, 0.948, 1.4, 1.23, and 1.005 g cm^{-3}, respectively. Other gamma-ray interactions with matter parameters were determined using the mass attenuation

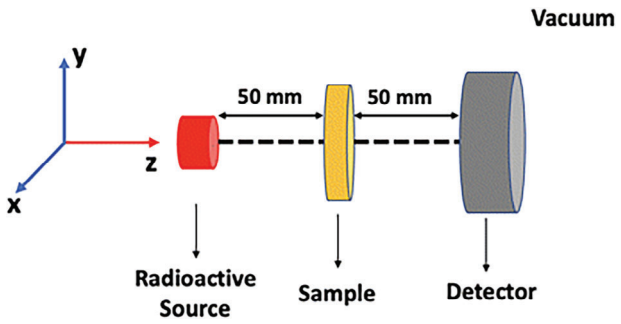

Figure 1. The geometry established for simulation studies.

coefficients obtained at twenty-five different photon energies in the energy range of 0.03 to 20 MeV with the WinXCOM[38] program, GEANT4[39] and FLUKA[40] simulation codes. μ/ρ is a parameter expressing the probability of interaction between a photon and a unit mass of matter in a unit area. The mixture rule was used to determine the μ/ρ parameter, which is a leading parameter and independent of the density of the material, by theoretical or simulation methods. According to this rule, the mass attenuation coefficient ($(\mu/\rho)_i$) of an element in the material was multiplied by its weight fraction (W_i), and this process was repeated for each element, and the μ/ρ of the material was determined from the sum of these. The mathematical representation of this process is as follows.[41]

$$(\mu/\rho)_{poly} = \sum_i W_i(\mu/\rho)_i \quad (1)$$

Equation (2) is used to calculate W_i, which indicates the weight fraction.

$$W_i = \frac{n_i A_i}{\sum_j n_j A_j} \quad (2)$$

In Equation (2), n and A represent the number of element and its atomic weight ith element in the material, respectively.

μ determined with the help of μ/ρ is a parameter that expresses the probability of the photon to interact with the unit thickness of the matter. This parameter varies according to the density of the matter and its solid, liquid, and gas form and is derived by multiplying the μ/ρ value of the polymer with its density. The parameters derived using μ are HVL, TVL, and MFP, respectively. These parameters express the required sample thicknesses for 50%, 90%, and 63.2% of the incident photon to interact with the matter, respectively, and can be derived with the following equations.[42,43]

$$HVL = ln2/\mu = 0.693/\mu \quad (3)$$

$$TVL = ln10/\mu = 2.303/\mu \quad (4)$$

$$MFP = 1/\mu \quad (5)$$

Another interaction parameter determined using μ/ρ is Z_{eff}. This is a parameter determined for materials containing at least two elements and varies with photon energy. The calculation

Table 1. Mass attenuation coefficients of the considered polymers.

Energy [MeV]	PP			PVA			EVA		
	WinXCOM	GEANT4	FLUKA	WinXCOM	GEANT4	FLUKA	WinXCOM	GEANT4	FLUKA
0.03	0.2707	0.2941	0.2709	0.3085	0.2930	0.3075	0.2992	0.2796	0.2991
0.04	0.2275	0.2074	0.2283	0.2363	0.2411	0.2365	0.2341	0.2210	0.2348
0.05	0.2084	0.1996	0.2107	0.2072	0.1991	0.2079	0.2075	0.1932	0.2093
0.06	0.1970	0.1891	0.2001	0.1916	0.1808	0.1926	0.1929	0.1854	0.1940
0.08	0.1823	0.1775	0.1847	0.1740	0.1675	0.1750	0.1760	0.1705	0.1770
0.1	0.1719	0.1683	0.1732	0.1628	0.1580	0.1638	0.1650	0.1601	0.1665
0.15	0.1534	0.1508	0.1536	0.1444	0.1414	0.1455	0.1466	0.1499	0.1472
0.2	0.1402	0.1384	0.1398	0.1316	0.1297	0.1328	0.1337	0.1344	0.1328
0.3	0.1217	0.1210	0.1214	0.1141	0.1134	0.1138	0.1160	0.1116	0.1154
0.4	0.1090	0.1089	0.1085	0.1021	0.1021	0.1019	0.1038	0.1029	0.1032
0.5	0.0995	0.0996	0.0999	0.0932	0.0934	0.0944	0.0948	0.0914	0.0949
0.6	0.0920	0.0924	0.0915	0.0862	0.0866	0.0879	0.0876	0.0886	0.0878
0.8	0.0808	0.0813	0.0798	0.0757	0.0761	0.0766	0.0769	0.0774	0.0764
1	0.0726	0.0730	0.0724	0.0681	0.0684	0.0671	0.0692	0.0696	0.0681
1.25	0.0649	0.0651	0.0639	0.0609	0.0611	0.0602	0.0619	0.0621	0.0616
1.5	0.0591	0.0591	0.0592	0.0554	0.0555	0.0557	0.0563	0.0563	0.0558
2	0.0506	0.0505	0.0507	0.0475	0.0474	0.0474	0.0483	0.0482	0.0476
3	0.0405	0.0402	0.0402	0.0381	0.0379	0.0384	0.0387	0.0385	0.0384
4	0.0344	0.0342	0.0344	0.0326	0.0324	0.0319	0.0331	0.0329	0.0329
5	0.0304	0.0302	0.0297	0.0290	0.0288	0.0283	0.0293	0.0292	0.0291
6	0.0276	0.0274	0.0273	0.0264	0.0262	0.0262	0.0267	0.0265	0.0270
8	0.0238	0.0236	0.0242	0.0231	0.0230	0.0230	0.0233	0.0231	0.0228
10	0.0215	0.0214	0.0220	0.0210	0.0209	0.0209	0.0211	0.0210	0.0212
15	0.0182	0.0181	0.0186	0.0182	0.0181	0.0178	0.0182	0.0182	0.0186
20	0.0166	0.0166	0.0173	0.0169	0.0169	0.0168	0.0168	0.0167	0.0173
Energy [MeV]	PVC			CR			PUR		
	WinXCOM	GEANT4	FLUKA	WinXCOM	GEANT4	FLUKA	WinXCOM	GEANT4	FLUKA
0.03	1.4919	1.3855	1.4875	1.1308	1.0443	1.0443	0.3035	0.2860	0.3031
0.04	0.7299	0.6661	0.7326	0.5795	0.5283	0.5283	0.2362	0.2312	0.2373
0.05	0.4559	0.4130	0.4567	0.3802	0.3461	0.3461	0.2089	0.1939	0.2097
0.06	0.3324	0.3008	0.3339	0.2897	0.2649	0.2649	0.1940	0.1838	0.1951
0.08	0.2298	0.2102	0.2310	0.2129	0.1976	0.1976	0.1767	0.1705	0.1794
0.1	0.1887	0.1751	0.1894	0.1810	0.1703	0.1703	0.1656	0.1612	0.1666
0.15	0.1486	0.1413	0.1496	0.1475	0.1416	0.1416	0.1471	0.1441	0.1472
0.2	0.1308	0.1265	0.1315	0.1312	0.1276	0.1276	0.1342	0.1321	0.1341
0.3	0.1110	0.1092	0.1107	0.1121	0.1106	0.1106	0.1163	0.1155	0.1163
0.4	0.0987	0.0980	0.0988	0.0999	0.0994	0.0994	0.1041	0.1040	0.1041
0.5	0.0898	0.0897	0.0913	0.0910	0.0909	0.0909	0.0950	0.0952	0.0963
0.6	0.0829	0.0831	0.0837	0.0840	0.0842	0.0842	0.0879	0.0883	0.0885
0.8	0.0727	0.0730	0.0724	0.0737	0.0741	0.0741	0.0772	0.0775	0.0752
1	0.0653	0.0656	0.0664	0.0662	0.0666	0.0666	0.0694	0.0698	0.0697
1.25	0.0584	0.0586	0.0585	0.0592	0.0595	0.0595	0.0620	0.0622	0.0616
1.5	0.0532	0.0533	0.0529	0.0539	0.0540	0.0540	0.0565	0.0565	0.0564
2	0.0459	0.0458	0.0456	0.0464	0.0465	0.0465	0.0484	0.0484	0.0493
3	0.0374	0.0372	0.0370	0.0376	0.0375	0.0375	0.0388	0.0387	0.0388
4	0.0326	0.0324	0.0321	0.0326	0.0324	0.0324	0.0332	0.0330	0.0334
5	0.0296	0.0294	0.0287	0.0294	0.0292	0.0292	0.0295	0.0293	0.0296
6	0.0275	0.0274	0.0271	0.0272	0.0270	0.0270	0.0268	0.0266	0.0271
8	0.0250	0.0249	0.0243	0.0243	0.0242	0.0242	0.0234	0.0233	0.0232

(*Continued*)

Table 1. (Continued)

Energy [MeV]	PP			PVA			EVA		
	WinXCOM	GEANT4	FLUKA	WinXCOM	GEANT4	FLUKA	WinXCOM	GEANT4	FLUKA
10	0.0236	0.0234	0.0232	0.0227	0.0226	0.0226	0.0212	0.0212	0.0216
15	0.0219	0.0218	0.0218	0.0207	0.0206	0.0206	0.0183	0.0183	0.0185
20	0.0214	0.0213	0.0213	0.0199	0.0198	0.0198	0.0169	0.0169	0.0177

process of Z_{eff} is determined by the atomic[44] and electronic[44] cross sections determined with the help of μ/ρ presented in previous studies and the Z_{eff} parameter is determined by the following equation.[44]

$$Z_{eff} = \sigma_{t,a}/\sigma_{t,e} \tag{6}$$

EBF and EABF are parameters related to the amount of energy stored or absorbed by the incident photon by interacting with the air and matter, respectively. These parameters were determined with the help of EpiXS program[45] for twenty-five different photon energies in the range of 0.015 to 15 MeV and eighteen different penetration depths in the range of 1 to 40 mfp.

In this program, EPICS2017,[46] which uses photo-atomic data from the ENDF/B-VIII[47] library, was preferred. There are known three basic processes for the calculation of EBF and EABF; i) determination of the equivalent atomic numbers of the material,[48] ii) determination of the Geometric-Progression fitting parameters,[49] and iii) obtaining the EBF and EABF results. EBF and EABF parameters are determined by the following equations.[50]

$$B(E,x) = 1 + \frac{b-1}{K-1}(K^x - 1) \; for \; K \neq 1 \tag{7}$$

$$B(E,x) = 1 + (b-1)\,x \; for \; K = 1 \tag{8}$$

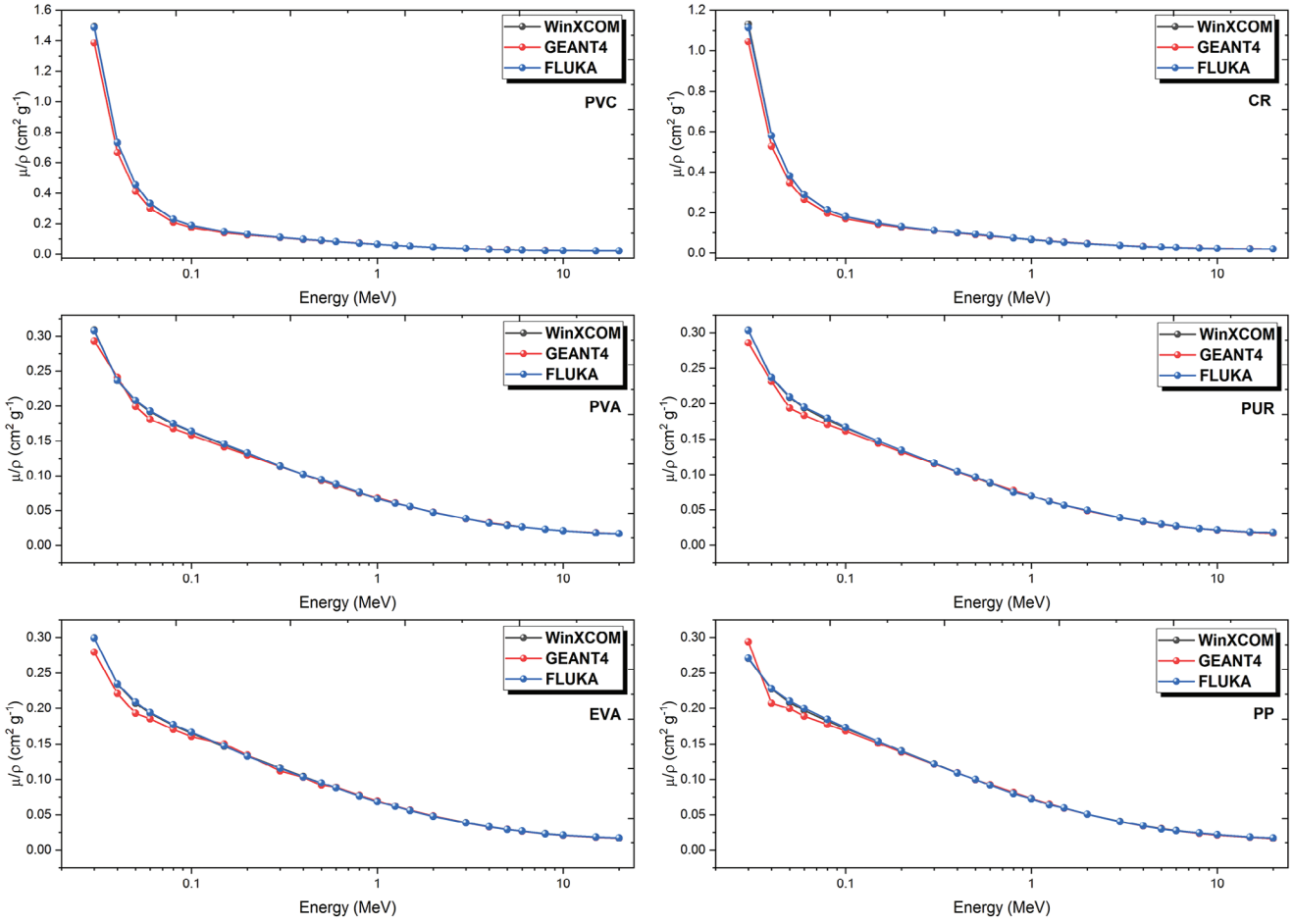

Figure 2. The comparative display of μ/ρ results versus photon energy for the studied polymers.

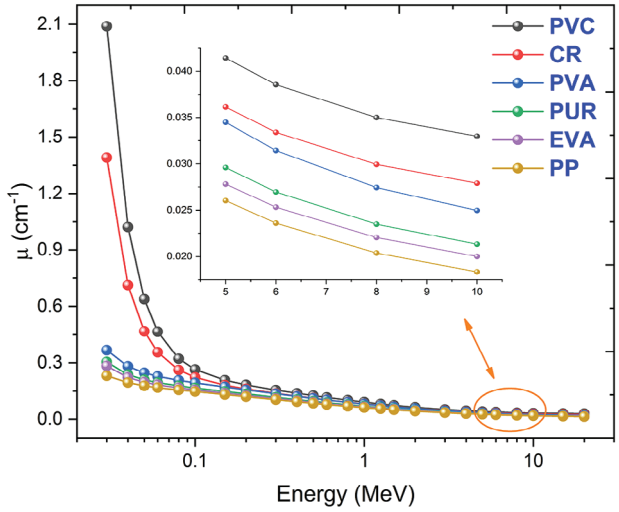

Figure 3. μ results versus photon energy for the studied polymers.

K in Equation (8) is calculated with the following equation.

$$K(E,x) = cx^{a} + d\frac{tanh\left(\frac{x}{X_K} - 2\right) - \tanh(-2)}{1 - \tanh(-2)} \quad for\ x \le 40\ mfp \quad (9)$$

In the above equations, a, b, c, d, and X_K represent the Geometric-Progression fitting coefficients at 1 mfp buildup factor, E represents the energy and x represents the penetration depth in mfp.

Kerma, which is an abbreviation for kinetic energy released per unit mass, is defined as the amount of released energy in the medium. For example, the Kerma relative to water parameter expresses the energy a photon leaves in the matter under examination compared to water. This is a parameter used by radiologists, especially in cancer diagnosis, and is determined

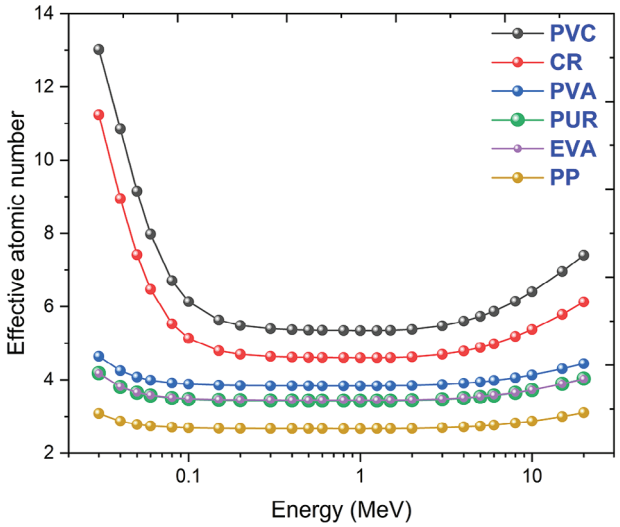

Figure 5. Z_{eff} results versus photon energy for the studied polymers.

with the help of the following equation.[51]

$$K = \Psi\left(\mu_{en}/\rho\right) = \frac{\left(\mu_{en}/\rho\right)_{poly}}{\left(\mu_{en}/\rho\right)_{X}} (X = air, water, ordinary\ concrete, lead\ glass) \quad (10)$$

In Equation (10), Ψ represents the energy fluence, while μ_{en}/ρ represents the mass-energy attenuation coefficient and was taken from the tables of Hubbell and Seltzer.[52]

The effective removal cross-section for fast neutrons parameter, which was calculated theoretically to investigate the interactions of the studied polymers with neutron particles, was a parameter related to the probability of the incoming neutron

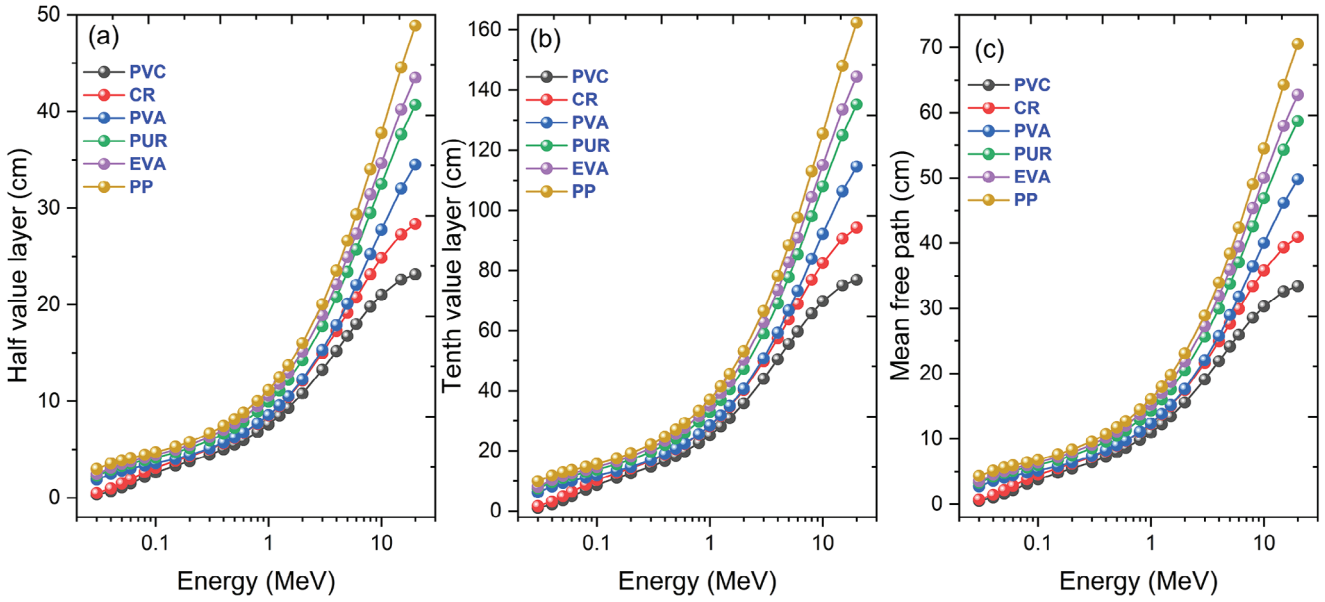

Figure 4. a) HVL b) TVL c) MFP results versus photon energy for the studied polymers.

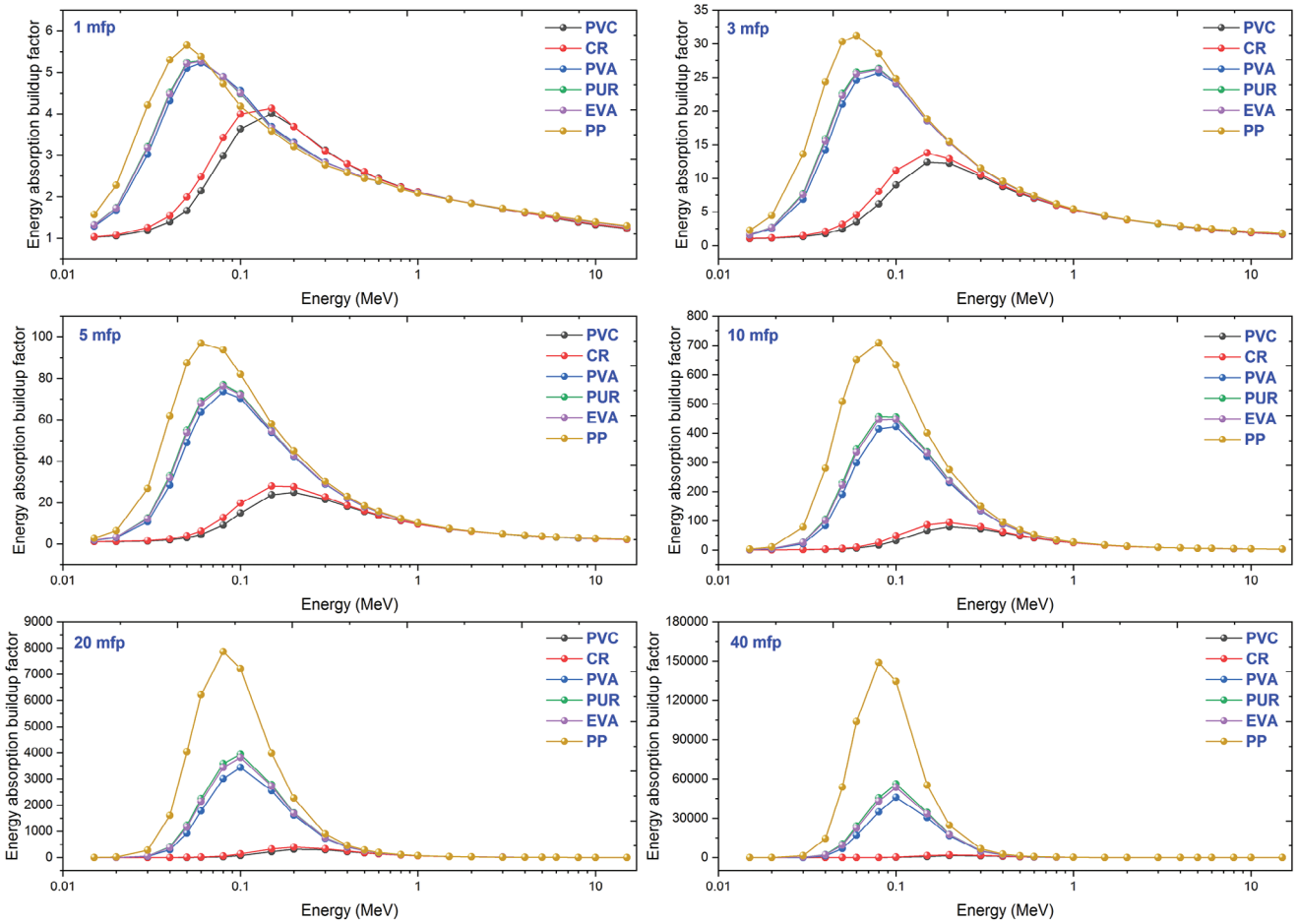

Figure 6. The variation of EABF results with photon energy at different penetration depths for the studied polymers.

particles to have a first collision with the matter and it is determined by Equation (11) for any mixture or compound.[53]

$$\Sigma_R = \sum_i \rho_i \left(\Sigma_R/\rho\right)_i \tag{11}$$

In the equation, $(\Sigma_R/\rho)_i$ represents the mass removal cross-section value of the ith element in the material, while ρ_i is the partial density of that element.

Partial neutron numbers passing through the polymers at different neutron energies, secondary radiations resulting from gamma and neutron interactions with polymers, total ionizing dose, and displacements-per-atom parameters were determined directly with FLUKA or GEANT4 codes.

2.2. Simulations Processes

The chosen Monte Carlo (MC) simulation tools for this study are the FLUKA and GEANT4 codes, as mentioned earlier. The simulation geometry is simple, as shown in **Figure 1**. A monoenergetic radiation source emits photons or neutrons only in the z-direction, and the medium is set as a vacuum to avoid interactions with air. The choice of vacuum medium allows the focus to remain solely on assessing the ionizing radiation interactions with the materials. The samples are first modeled in the GEANT4 simulation package, using their chemical compositions and dimensions. To simulate the interactions between photons and the selected polymer materials, 10 000 000 photon particles are directed toward each sample at a 90-degree angle. From these simulations, parameters such as μ/ρ, μ, HVL, TVL, and MFP are determined based on the number of transmitted particles through the material.

Similarly, the FLUKA simulation package, interfaced with the FLAIR, is used to calculate particle transmission and interactions with matter. In FLUKA, each sample is modeled separately. The radiation type is set to "Photon" using the "BEAM" command, and the radiation source location is defined with the "BEAMPOS" option. The geometry of the sample is established using the "GEOBEGIN" card, while material properties and densities are specified using the "MATERIAL" and "COMPOUND" cards. The "USRBDX" card is then used to determine the number of photon particles passing through the sample. As in GEANT4, the FLUKA simulations also involve sending 10 000 000 monoenergetic photon particles onto the samples.

In addition, neutron interactions with the polymer materials are simulated and evaluated with the help of FLUKA and GEANT4 codes. The simulation geometry is exactly the same as the photon interactions section. First of all, the simulated

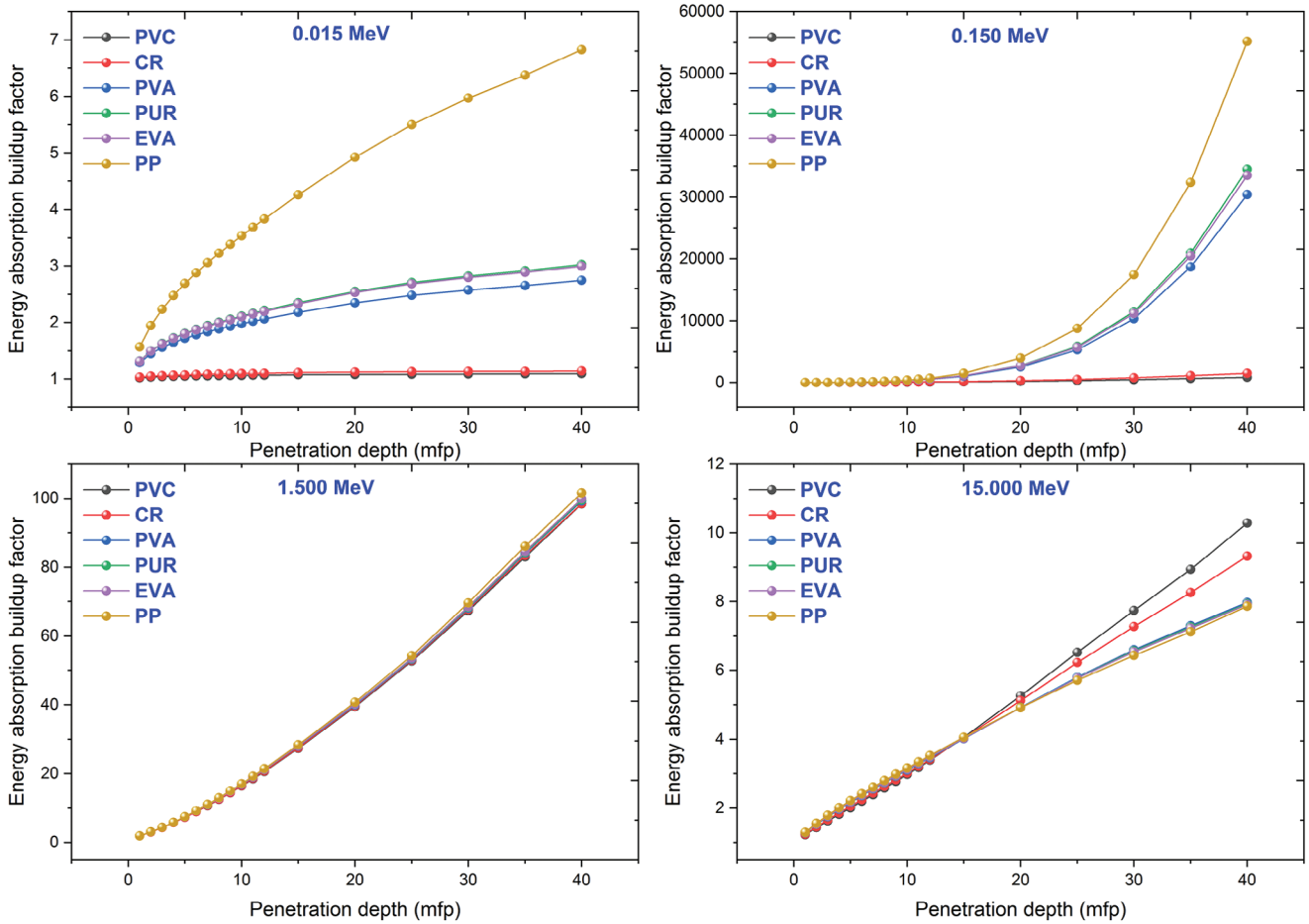

Figure 7. The variation of EABF results with penetration depth at different photon energies for the studied polymers.

numbers of transmitted neutrons are determined, and the ratio of transmitted to initial particles is obtained. Here, three different neutron energies are considered and 10 000 000 monoenergetic neutrons are simulated. The chosen neutron energies are 0.025 eV (thermal neutrons), 100 eV (slow neutrons), and 4.5 MeV (fast neutrons). With the help of GEANT4, the secondary radiations due to the primary radiation interactions are further determined with their average energies.

DPA and TID are critical metrics for assessing radiation-induced damage in materials, providing insight into the radiation interactions. These parameters are evaluated using the FLUKA simulation tool. The "USRBIN" card in the FLAIR interface is employed to calculate both TID and DPA values. For each sample, simulations are conducted at various photon or neutron energies to determine the corresponding TID and DPA values. To visualize and better understand how radiation interacts with the material, 2D TID graphs are additionally drawn.

3. Results and Discussion

The study examines materials such as PP, EVA, PVA, PVC, CR, and PUR, which play significant roles in the nuclear energy sector due to their properties like radiation resistance, thermal stability, and chemical resistance. While these materials are valuable in certain applications, their radiation resistance and interactions deserve further investigation. In this study, the gamma-ray interactions with the chosen materials are first evaluated and presented, beginning with a comparison of their mass attenuation coefficients. **Table 1** presents the numerical results obtained using WinXCOM, GEANT4, and FLUKA tools. With a maximum deviation of ≈8% between the tools, it can be concluded that there is strong consistency among them. **Figure 2** illustrates the numerical results obtained across a broad gamma energy range, varying from 30 keV to 20 MeV. Different trends in μ/ρ values, as shown in Figure 2, are mainly attributed to differences in their distinct chemical compositions, which affect their interaction with gamma rays. For example, PVC contains chlorine (Z = 17), which results in a higher μ/ρ at lower energies due to the photoelectric effect. In contrast, polymers such as PP and PVA, mainly composed of carbon, hydrogen, and oxygen (low-Z elements), exhibit lower μ/ρ values. Polymers with higher mass attenuation coefficients at lower energies, like PVC and CR, are more effective for medical radiation shielding and low-energy gamma sources. Meanwhile, materials like PUR and EVA offer flexibility and durability, making them better suited for intermediate to high-energy applications, such as in industrial

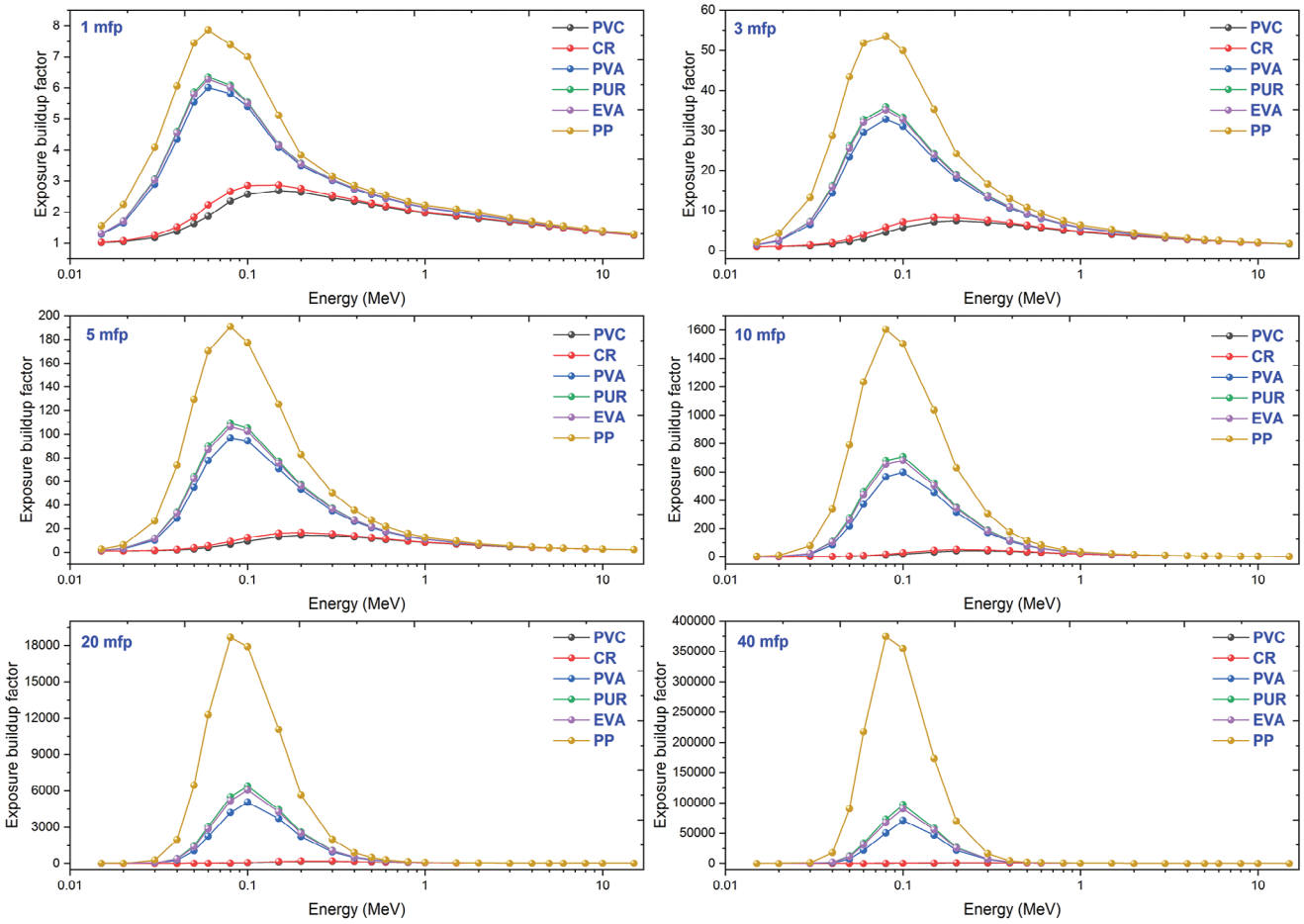

Figure 8. The variation of EBF results with photon energy at different penetration depths for the studied polymers.

radiation environments or in multilayer shielding systems. Additionally, the linear attenuation coefficient is a key parameter in assessing gamma-ray interactions. **Figure 3** presents the calculated values, comparing each material against the others. Here, the curves are plotted using only the FLUKA results. According to this graphical comparison, PVC appears as the polymer that interacts most with gamma rays, while PP is identified as the polymer that interacts least with gamma rays. HVL, TVL, and MFP graphs of the materials can offer deeper insights into their gamma-ray interactions. HVL (TVL) simply identify the required material thickness to reduce the initial radiation intensity to its half (one-tenth). Therefore, smaller HVL and TVL values indicate greater efficiency in gamma-ray attenuation. Similarly, the material with the lowest MFP value among those considered presents the highest gamma-ray attenuation capability. With the provided information, the HVL, TVL, and MFP graphs shown in **Figure 4**, derived from FLUKA results, could be additionally considered. Based on these results, it is evident that PVC exhibits superior gamma-ray attenuation performance, while PP demonstrates comparatively poorer gamma-ray interactions.

In addition to the parameters presented above, **Figure 5** represents the effective atomic number of the materials, a concept commonly used in radiation physics to analyze how photons (such as X-rays or gamma rays) and charged particles interact with material. A higher Z_{eff} indicates a greater ability of the material to interact with incoming photons. In this context, the highest Z_{eff} values are observed for PVC and CR materials, suggesting that they have the highest photon interaction rates among the materials considered. Here, it should be underlined that the linear attenuation coefficient and the effective atomic number are closely related, with materials that have higher Z_{eff} typically showing greater μ values, resulting in more efficient gamma-ray attenuation. As it is already found that PVC and CR have greater Z_{eff} and μ values. However, this relationship varies across different gamma-ray energy ranges. For instance, in the energy region where the photoelectric effect dominates, the relationship could be described as $\mu \propto (Z_{eff})^{4-5}\ E^{-3.5}$. In contrast, when Compton scattering is dominant, it follows $\mu \propto Z_{eff}\ E^{-1}$, and for pair production, the relationship becomes $\mu \propto Z_{eff}\ \ln(E^2)$.

Figures 6 and **7** illustrate the variations in energy absorption buildup factor (EABF) with photon energy at different penetration depths, and with penetration depth at different photon energies, respectively. In the energy range of 0.01–0.1 MeV, PP exhibits the highest EABF, reflecting a strong contribution from the photoelectric effect. In the intermediate energy range of 0.1–1 MeV, where Compton scattering dominates, PP still maintains the highest EABF, indicating that its composition favors continued energy absorption through scattered photons. However,

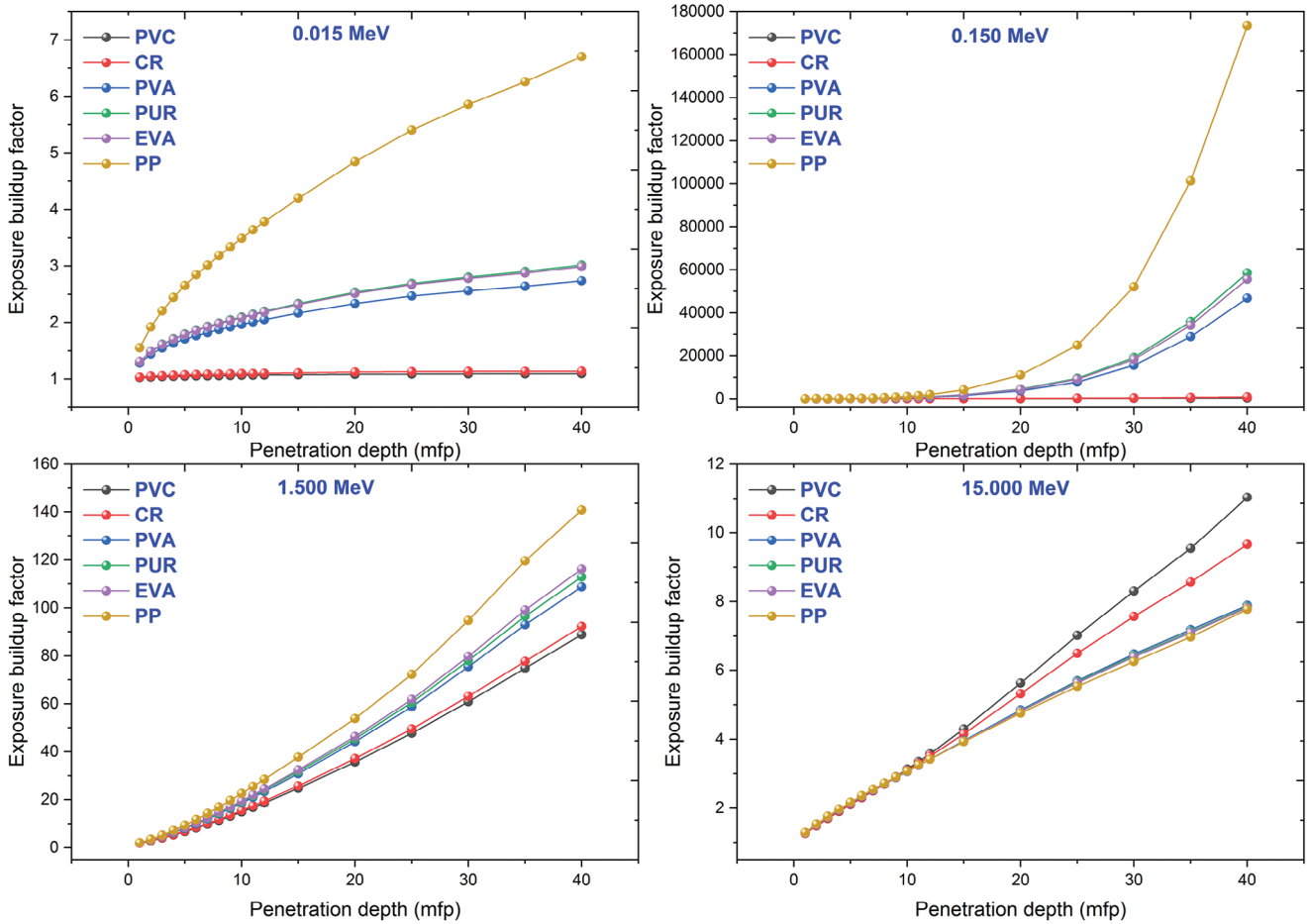

Figure 9. The variation of EBF results with penetration depth at different photon energies for the studied polymers.

in the high-energy range of 1–10 MeV, the EABF values across all materials become more similar, as pair production becomes more prominent. Throughout these energy regions, PVC and CR show the lowest EABF values, indicating it is less effective at energy absorption compared to the other materials.

Figures 8 and 9 show the variation of exposure buildup factor (EBF) results with photon energy at different penetration depths and with penetration depth at different photon energies, respectively. The EABF and EBF results are consistent in terms of trends and the ranking of materials based on their photon interaction behaviors. PP has the highest value of EBF, while PVC could be identified with the lowest value of EBF.

Additionally, evaluating the Kerma (Kinetic Energy Released per Unit Mass) values of the considered materials can provide a more comprehensive understanding of photon interactions. Generally, a material with a higher Kerma relative to air, water, concrete, or lead glass is more effective at absorbing radiation energy. In this context, **Figure** 10 presents the Kerma values relative to air, water, ordinary concrete, and lead glass versus photon energy for the studied polymers. Among these categories, PVC consistently shows higher Kerma values for most photon energies, indicating that PVC is more effective at absorbing radiation energy. According to Figure 10, it is seen that PVC polymer interacts with more gamma radiation in air, water, ordinary concrete and lead glass environments than other polymers, and the kinetic energy released per unit mass in PVC polymer in these environments is greater than the others.

Another research point of this study is the interaction of the studied polymers with neutrons. For this purpose, effective removal cross-section values were theoretically calculated. These calculations are further supported by the values obtained using GEANT4 and FLUKA simulation tools. The obtained results are presented in **Table** 2. Here, it should be underlined here that a greater effective removal cross-section indicates greater neutron interactions with materials. Based on the calculated cross-section values, the ranking of neutron interactions from worst to best is as follows: PVC, CR, EVA, PUR, PVA, and PP. Table 2 also presents simulation results for the ratio of transmitted neutrons to the initial number of neutrons, with these simulations conducted on samples with a 1 cm thickness and 4.5 MeV neutron energy. Here, a smaller ratio indicates higher interaction. The order derived from the MC simulations aligns with the order determined by the effective removal cross-section. Finally, it should be noted that there is significant consistency between the GEANT4 and FLUKA simulations.

The investigation of neutron interactions with the considered materials has been advanced by incorporating analysis of secondary radiations. To ensure a comprehensive analysis, different

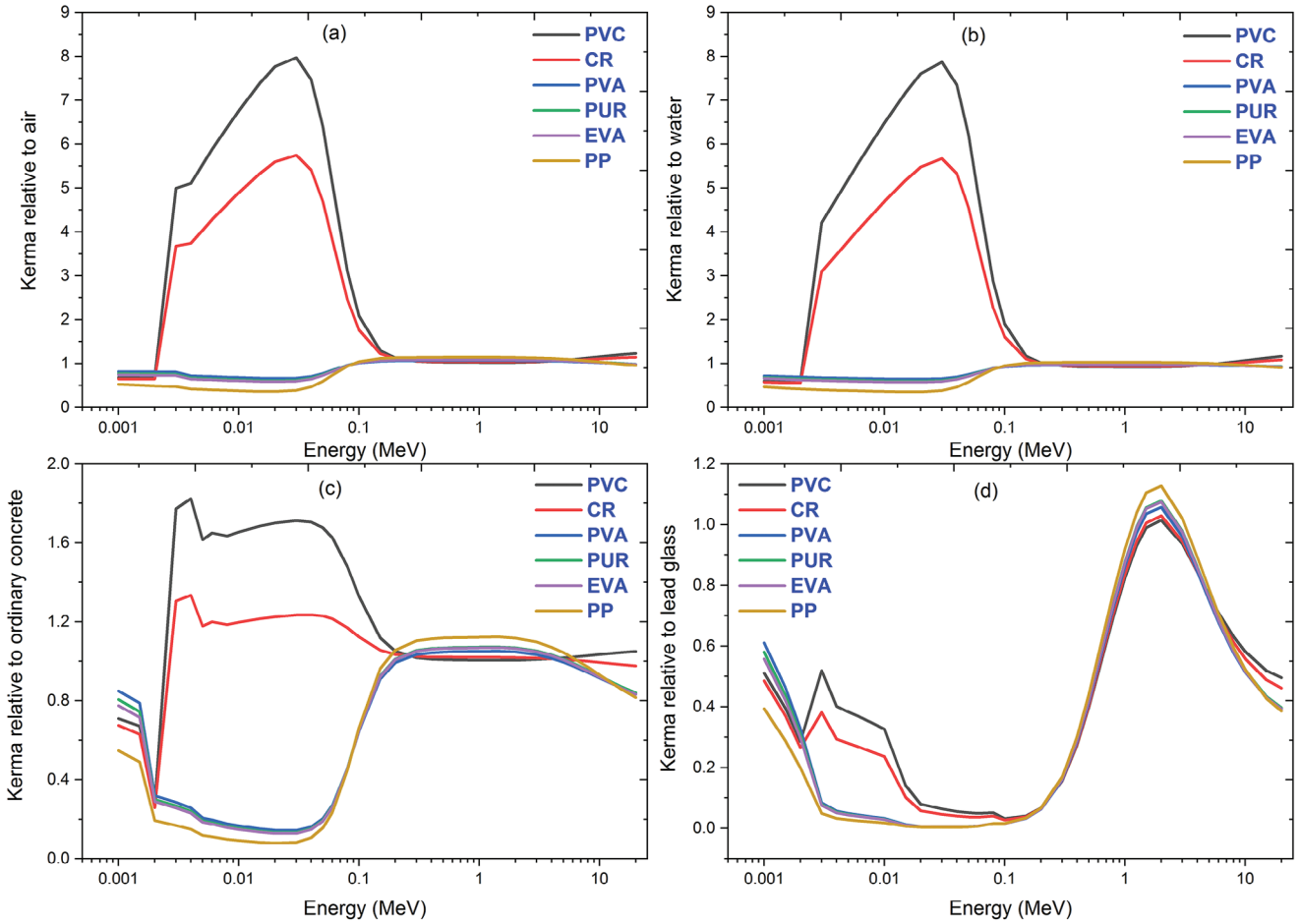

Figure 10. a) Kerma relative to air b) Kerma relative to water c) Kerma relative to ordinary concrete and d) Kerma relative to lead glass results versus photon energy for the studied polymers.

neutron energies is considered, as the materials interact not only with monoenergetic neutrons but also with neutrons at various energies. In this context, fast (4.5 MeV), slow (100 eV), and thermal (0.025 eV) neutrons are considered. Based on the assessment of transmitted neutrons, the performance of all samples in interacting with neutrons is ranked from best to worst for thermal, slow, and fast neutrons, respectively. For the interactions of primary slow and thermal neutrons with the selected polymers, no secondary neutrons are generated. However, when fast neutrons interact with these materials, secondary neutrons with an average energy greater than 1 MeV are produced. The highest number of secondary neutrons is observed in the PVC sample, followed by the CR polymer. Across all neutron categories, PVC polymer also produces the highest number of secondary gamma rays, with the CR sample following closely behind. In other words, according to the simulation results presented in **Table 3**, PVC and CR polymers are the least advantageous choices due to their higher production of secondary neutrons and gamma rays.

Table 2. Effective removal cross-section values and I/I_0 ratios (GEANT4 and FLUKA) for the samples.

Sample Code	I/I_0 [GEANT4]	I/I_0 [FLUKA]	Effective Removal Cross Section [cm^{-1}]
PP	0.8267	0.8257	0.1102
PVA	0.8472	0.8443	0.1013
EVA	0.8533	0.8529	0.0909
PVC	0.8594	0.8576	0.0875
CR	0.8555	0.8556	0.0878
PUR	0.8493	0.8479	0.0973

Assessing structural damage to materials caused by radiation irradiation is crucial to determine the impact of long-term use of construction materials in nuclear reactors. Various effects and parameters are key to studying how materials behave under irradiation, and FLUKA is equipped to predict some of these factors. In this sense, Total Ionizing Dose and Displacement per Atom values are evaluated for the chosen materials. **Table 4** summarizes the obtained TID and DPA results for various gamma-ray energies. It is clearly observed that TID and DPA values increase with the increase of gamma-ray energy. Up to 1 MeV, the lowest TID value belongs to PVC, which is followed by CR. For 10 and 20 MeV gamma-ray energies, the lowest TID value is observed for PP, which is followed by EVA. At 0.001 and 0.1 MeV energies,

Table 3. Neutron interactions with materials and the number of generated secondary particles for fast, slow and thermal neutrons.

Fast Neutrons						
Sample Code	Primary Neutrons	Transmitted Neutrons	Number of Secondary Gammas	Average Energy of Secondary Gammas [MeV]	Number of Secondary Neutrons	Average Energy of Secondary Neutrons [MeV]
PP	10000000	8267121	79	1.9729	4	1.1162
PVA	10000000	8472484	16596	0.7181	193	1.6747
EVA	10000000	8593823	9830	0.7203	130	1.6029
PVC	10000000	8532700	203992	1.7878	88675	1.4492
CR	10000000	8555096	127023	1.7903	55209	1.4415
PUR	10000000	8493417	31849	0.9143	5126	1.0139
Slow Neutrons						
Sample Code	Primary Neutrons	Transmitted Neutrons	Number of Secondary Gammas	Average Energy of Secondary Gammas [MeV]	Number of Secondary Neutrons	Average Energy of Secondary Neutrons [MeV]
PP	10000000	1854539	1931	2.2427	0	0
PVA	10000000	2877890	1566	2.2413	0	0
EVA	10000000	3002688	1554	2.2635	0	0
PVC	10000000	3409705	53425	3.5788	0	0
CR	10000000	3368849	33871	3.5387	0	0
PUR	10000000	2,5204,18	1966	2.7250	0	0
Thermal Neutrons						
Sample Code	Primary Neutrons	Transmitted Neutrons	Number of Secondary Gammas	Average Energy of Secondary Gammas [MeV]	Number of Secondary Neutrons	Average Energy of Secondary Neutrons [MeV]
PP	10000000	626713	84693	2.2500	0	0
PVA	10000000	1608049	79127	2.2592	0	0
EVA	10000000	1590647	77955	2.2542	0	0
PVC	10000000	1326446	5532333	3.5983	0	0
CR	10000000	1442026	3559680	3.5949	0	0
PUR	10000000	1166836	88599	2.8106	0	0

PVC exhibits the lowest DPA value, indicating less radiation-induced damage to the material. In contrast, PP shows the highest DPA values at these two energies. However, at 1, 10, and 20 MeV energies, PP has the lowest DPA values compared to the other materials considered.

Table 4. TID and DPA values of gamma-ray interactions for studied polymers.

TID [GeV g^{-1}] x 10^{-12}						
Energy [MeV]	PP	PVA	EVA	PVC	CR	PUR
0.001	9.3355	6.7074	8.4197	5.7013	6.4893	7.9421
0.01	292.40	210.08	263.71	178.57	203.25	248.76
1	720.97	696.16	734.54	683.13	699.18	729.42
10	56065	74397	59362	105840	88828	64187
20	48382	68002	53548	106520	87895	58008
DPAx 10^{-30}						
Energy [MeV]	PP	PVA	EVA	PVC	CR	PUR
0.001	0.030353	0.015107	0.021475	0.0092623	0.012051	0.020540
0.01	0.054137	0.030042	0.041448	0.021651	0.026260	0.039765
1	142.87	175.09	163.60	153.71	159.65	161.08
10	261.34	537.38	377.38	1015.2	731.47	403.46
20	240.98	531.78	365.84	1143.4	796.60	392.27

Similarly, TID and DPA values were obtained for neutron interactions using the FLUKA MC simulation tool, as presented in **Table 5**. PVC and CR exhibit significantly higher TID values compared to other materials, indicating they are more sensitive to ionizing radiation from thermal neutrons. Conversely, PP, PVA, and EVA show much lower TID values, suggesting better resistance to thermal neutron radiation. TID values for fast neutrons are the highest among all neutron types, with PP suffering the most ionizing damage. PUR and EVA also exhibit high TID values, indicating significant sensitivity to fast neutron radiation. PVC and PUR also show much higher DPA values, reflecting greater displacement damage from thermal neutrons, consistent with their higher TID values. In contrast, PP, PVA, and EVA have lower DPA values, indicating less structural damage from thermal neutrons. Fast neutrons cause the highest DPA values across all materials, with PVC showing the highest value, indicating it experiences the most displacement damage. PP and PVA also have notably high DPA values, suggesting substantial radiation-induced structural damage. With increasing neutron energy, greater radiation damage is generally expected. However, from thermal to slow neutrons, both TID and DPA values decrease. The decrease in TID and DPA values from thermal to slow neutrons can be at-

Table 5. TID and DPA values of neutron interactions for studied polymers.

TID [GeV g^{-1}] x 10^{-8}						
Neutron	PP	PVA	EVA	PVC	CR	PUR
Thermal	1.0042	0.64901	0.63150	28.024	20.705	7.9990
Slow	0.1387	0.05724	0.058096	1.7681	1.2124	0.68210
Fast	96.001	51.760	62.276	37.13	42.726	69.003
DPA x 10^{-25}						
Neutron	PP	PVA	EVA	PVC	CR	PUR
Thermal	0.035567	0.027619	0.029739	1.324	0.95344	1.7215
Slow	0.0042816	0.0018810	0.0020123	0.084034	0.056610	0.14337
Fast	3.8786	8.1390	6.6635	12.908	9.8501	6.7367

tributed to changes in neutron interaction cross-sections, moderation effects, and resonance peaks. Thermal neutrons often have higher interaction probabilities and energy that match closely with material nuclei, leading to greater ionizing damage and displacement. As neutrons slow down, their interaction characteristics may change, resulting in reduced damage indicators. Further investigation into material properties is needed to fully explain these variations.

TID graphs in 2D were also obtained using FLUKA simulation package. First of all, the definition of the simulation geometry should be clearly explained here. **Figure** 11a shows the geometry, where the considered material is located in a coordinate system. The radiation source is located on z-axis, which emits gamma rays (or neutrons) in only +z direction. The radiation hits the material surface at an angle of 90^0. Figure 11b–d presents 2D TID graph of neutron interactions for only PP material. The graphs of the remaining materials are like each other. Therefore, only one material is chosen for the showcase. As the energy of the radiation increases, the overall TID values decrease. This behavior is typically expected because higher energy radiation tends to pass through the material with less interaction, leading to less energy deposition and, therefore, lower TID. The graphs also show

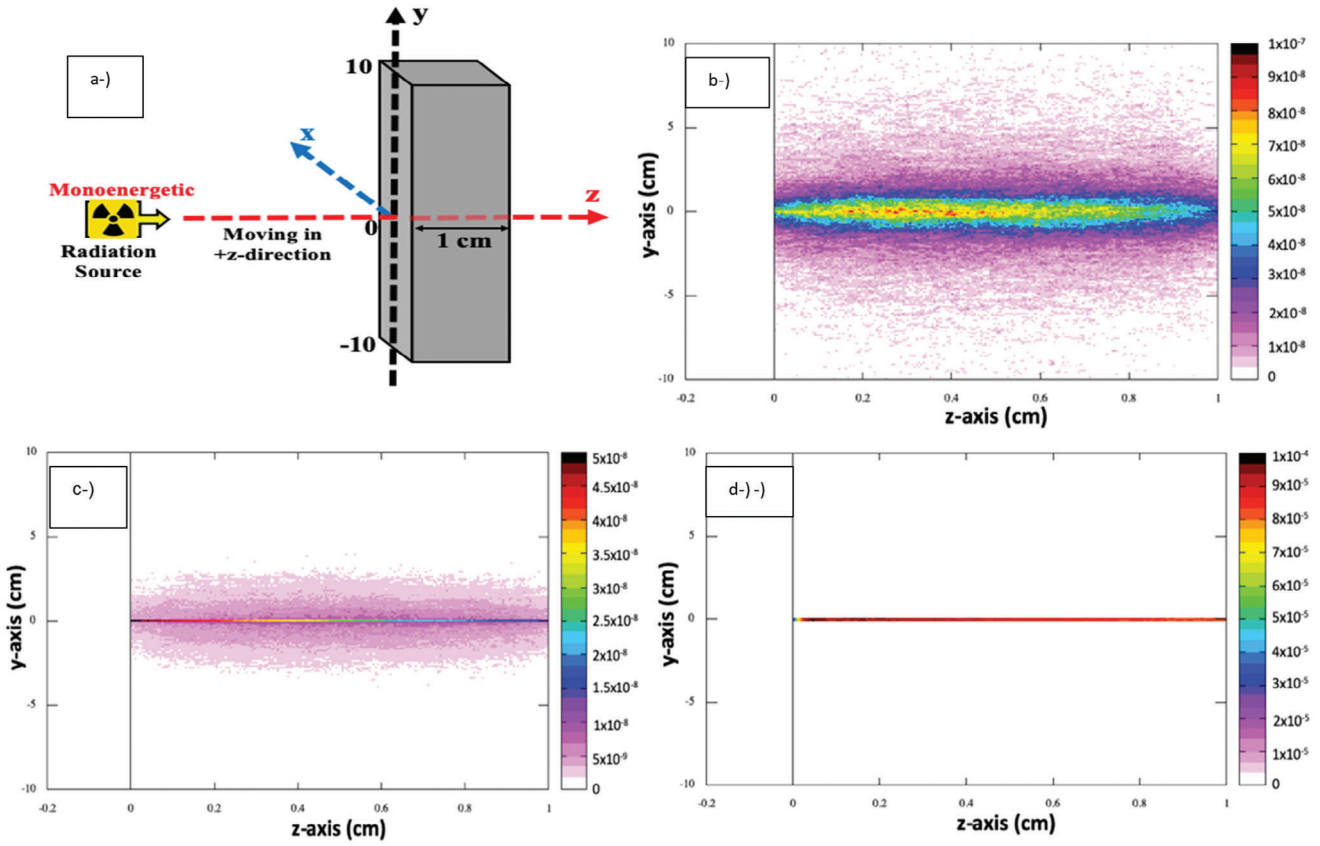

Figure 11. a) Schematic of the simulation setup and 2D TID distribution for b) thermal, c) slow, and d) fast neutrons interactions with PP material.

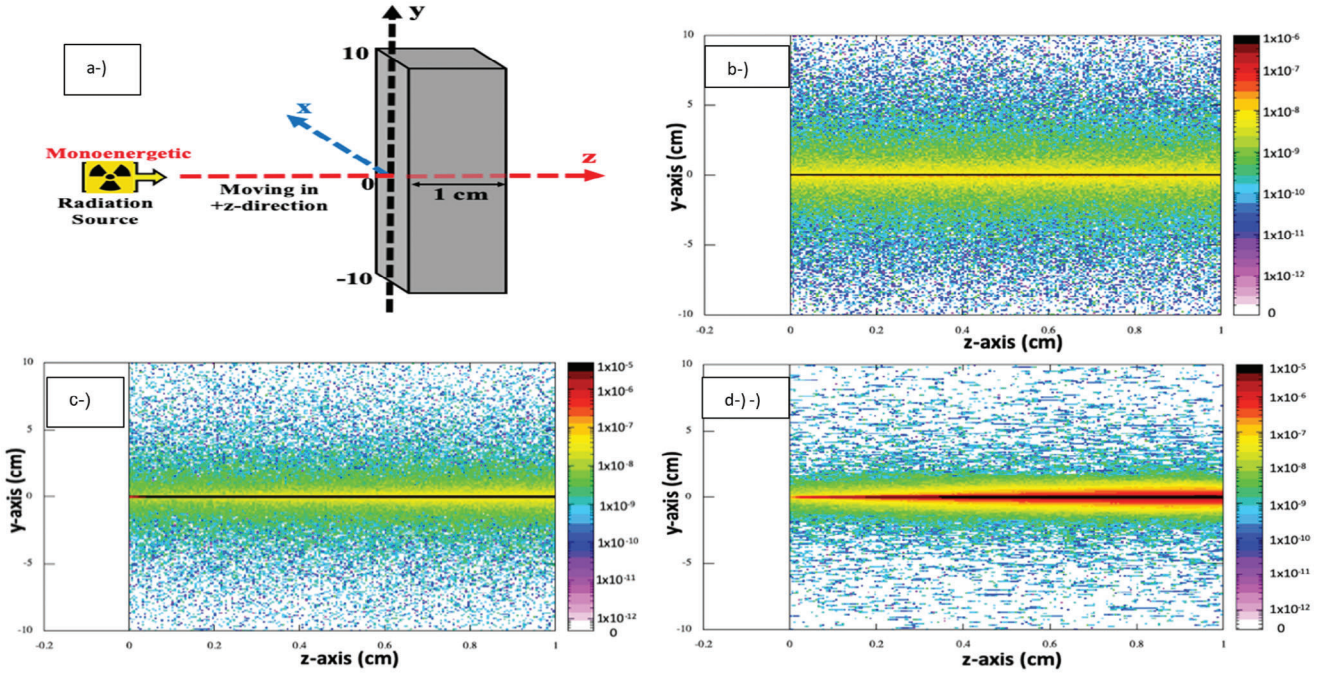

Figure 12. a) Schematic of the simulation setup and 2D TID distribution for gamma-ray interactions with PP material. The TID distributions are shown for gamma-ray energies of b) 50 keV, c) 500 keV, and d) 5 MeV.

that as the radiation energy increases, the spatial distribution of TID becomes narrower. This suggests that higher energy radiation has a more focused energy deposition along its path, likely because it interacts less frequently with the material, leading to fewer scatterings.

Figure 12 presents a similar figure for gamma-ray interactions. The TID distribution at 50 keV Figure 12b shows a relatively widespread in the y-axis direction. This indicates that lower-energy gamma rays are interacting more extensively with the polymers, resulting in a broader lateral scattering. The distribution at 500 keV shows some narrowing compared to 50 keV, but it still covers a significant portion of the material in the y-direction. This suggests that while 500 keV gamma rays interact less frequently than 50 keV rays, they still deposit energy over a relatively large area. At 5 MeV, the TID distribution becomes very focused and narrow, concentrated in the middle of the plot along the z-axis. This reflects the behavior of high-energy gamma rays, which interact less frequently with the material, resulting in a much more localized dose distribution. The minimal scattering at this energy leads to a narrow band, consistent with high-energy photons penetrating the material with little deviation.

4. Conclusion

This study presents a comprehensive evaluation of the gamma-ray and neutron interactions with various polymers, including PP, EVA, PVA, PVC, CR, and PUR, using a combination of theoretical calculations and Monte Carlo simulations. The findings offer valuable insights into the radiation interaction performance of these materials, highlighting their potential advantages and limitations.

The analysis of mass attenuation coefficients, linear attenuation coefficients, and derived parameters such as HVL, TVL, and MFP demonstrates that PVC more interacts with gamma radiation than the others studied polymers, with consistently highest/lower values across all energy ranges. Conversely, PP exhibits the lowest gamma-ray attenuation capabilities. The strong agreement between results from WinXCOM, GEANT4, and FLUKA highlight the reliability of the findings, with a maximum deviation of only 8% among the used tools. For neutron interactions, the effective removal cross-section values and the ratio of transmitted neutrons to initial neutrons indicate that PP provides the highest neutron interaction performance, followed by PVA, EVA, PUR, CR, and PVC. The consistency between GEANT4 and FLUKA simulation results supports the robustness of these conclusions. The analysis of secondary neutron and gamma-ray production reveals that PVC and CR generate the highest quantities of secondary radiation, making them less favorable for applications requiring minimal secondary radiation.

The investigation into radiation-induced structural damage using Total Ionizing Dose and Displacement per Atom metrics reveals that materials like PP, PVA, and EVA exhibit superior resistance to radiation damage compared to PVC and CR. The TID and DPA values increase with gamma-ray and neutron energy, with PP showing the lowest TID and DPA values at lower energies but experiencing significant damage from fast neutrons. Conversely, PVC and CR are more sensitive to thermal and fast neutron irradiation, indicating higher potential for structural damage in high-radiation environments.

In summary, PVA and PP emerge as the most promising materials for gamma-ray and neutron interactions, respectively, with PVC offering superior gamma attenuation and PP demonstrating the best overall neutron interaction performance. However,

the relation between radiation interactions and structural damage sensitivity should be carefully considered for specific applications. Future research should focus on further exploring the long-term effects of radiation exposure on these materials and the development of advanced composites that balance effective radiation interactions with minimal secondary radiation and structural damage.

Conflict of Interest

The authors declare no conflict of interest.

Data Availability Statement

The data that support the findings of this study are available from the corresponding author upon reasonable request.

Keywords

neutron interaction, photon interaction, polymers, radiation damage, secondary radiation

Received: August 30, 2024
Revised: October 16, 2024
Published online: November 6, 2024

[1] N. S. Kostyukov, T. Y. Eranskaya, *At. Energy* **2001**, *90*, 169.
[2] I.I. White, G. Von, R. Tandon, L. M. Serna, M. C. Celina, R. Bernstein, *An Overview of Basic Radiation Effects on Polymers and Glasses*, Sandia National Lab. (SNL-NM), Albuquerque **2013**.
[3] (Eds.: E. Reichmanis, C. W. Frank, J. H. O'Donnell, D. J. T. Hill), *Irradiation of Polymeric Materials*, American Chemical Society, Washington, DC **1993**, Ch. 1.
[4] P. Singh, R. Kumar, (Eds: V. Kumar, B. Chaudhary, V. Sharma, K. Verma) *Radiation Effects in Polymeric Materials*, Springer, Cham **2019**, Ch. 1.
[5] J. R. Laghari, A. N. Hammoud, *IEEE Trans. Nucl. Sci.* **1990**, *37*, 1076.
[6] I. Ishigaki, F. Yoshii, *Radiat. Phys. Chem.* **1992**, *39*, 527.
[7] H. Kudoh, T. Sasuga, T. Seguchi, *Radiat. Phys. Chem.* **1996**, *48*, 545.
[8] S. D. Bruck, E. P. Mueller, *J. Biomed. Mater. Res.* **1988**, *22*, 133.
[9] J. Verdu, *J. Macromol. Sci., Part A: Pure Appl.Chem.* **1994**, *31*, 1383.
[10] T. Sasuga, M. Hagiwara, *Polym* **1987**, *28*, 1915.
[11] H. C. Manjunatha, *Radiat. Phys. Chem.* **2017**, *137*, 254.
[12] N. M. Nagaraja, H. C. Manjunatha, L. Seenappa, K. N. Sridhar, H. B. Ramalingam, *Radiat. Prot. Environ.* **2019**, *42*, 150.
[13] M. I. Sayyed, M. Y. AlZaatreh, K. A. Matori, H. A. A. Sidek, M. H. M. Zaid, *Results Phys* **2018**, *9*, 585.
[14] R. Mirji, B. Lobo, *Radiat. Phys. Chem.* **2017**, *135*, 32.
[15] V. P. Singh, S. P. Shirmardi, M. E. Medhat, N. M. Badiger, *Vacuum* **2015**, *119*, 284.
[16] O. Gurler, U. T. Akar, *Acta Phys. Pol. A* **2016**, *130*, 236.
[17] N. Nagaraja, H. C. Manjunatha, L. Seenappa, K. V. Sathish, K. N. Sridhar, H. B. Ramalingam, *Indian J. Pure Appl. Phys.* **2022**, *58*, 271.
[18] N. Nagaraja, H. C. Manjunatha, Y. S. Vidya, L. Seenappa, K. N. Sridhar, P. D. Gupta, *Radiat. Phys. Chem.* **2022**, *199*, 110310.
[19] N. Kucuk, M. Cakir, N. A. Isitman, *Radiat. Prot. Dosim.* **2013**, *153*, 127.
[20] N. Nagaraja, K. N. Sridhar, H. C. Manjunatha, Y. S. Vidya, L. Seenappa, P. D. Gupta, H. B. Ramalingam, *Prog. Nucl. Energy* **2022**, *144*, 104044.
[21] R. R. Bhosale, C. V. More, D. K. Gaikwad, P. P. Pawar, M. N. Rode, *Nucl. Technol. Radiat. Prot.* **2017**, *32*, 288.
[22] Y. Elmahroug, B. Tellili, C. Souga, *Ann. Nucl. Energy* **2014**, *63*, 619.
[23] C. V. More, H. Alavian, P. P. Pawar, *Appl. Radiat. Isot.* **2021**, *176*, 109884.
[24] M. R. Kaçal, F. Akman, M. I. Sayyed, *Nucl. Eng. Technol.* **2019**, *51*, 818.
[25] C. V. More, H. Alavian, P. P. Pawar, *J. Non-Cryst. Solids* **2020**, *546*, 120277.
[26] M. T. Alabsy, J. S. Alzahrani, M. I. Sayyed, M. I. Abbas, D. I. Tishkevich, A. M. El-Khatib, M. Elsafi, *Mater* **2021**, *14*, 5051.
[27] M. I. Sayyed, *Chin. J. Phys.* **2016**, *54*, 408.
[28] M. S. Al-Buriahi, C. Eke, S. Alomairy, A. Yildirim, H. I. Alsaeedy, C. Sriwunkum, *Polym. Adv. Technol.* **2021**, *32*, 2386.
[29] N. Nagaraja, H. C. Manjunatha, L. Seenappa, K. N. Sridhar, H. B. Ramalingam, *Radiat. Phys. Chem.* **2020**, *171*, 108723.
[30] M. Saiyad, N. M. Devashrayee, R. K. Mevada, *Polym. Compos.* **2014**, *35*, 1263.
[31] F. Özkalaycı, M. R. Kaçal, H. Polat, O. Agar, N. Almousa, F. Akman, *Radiochim. Acta* **2022**, *110*, 393.
[32] M. F. Turhan, F. Akman, M. R. Kaçal, H. Polat, İ. Demirkol, *Appl. Radiat. Isot.* **2023**, *191*, 110568.
[33] H. Özdoğan, Y. A. Üncü, F. Akman, H. Polat, M. R. Kaçal, *Polym.* **2024**, *16*, 1778.
[34] F. Akman, O. Kilicoglu, H. Ogul, H. Ozdogan, M. R. Kaçal, H. Polat, *Radiat. Phys. Chem.* **2024**, *219*, 111682.
[35] F. Akman, H. Ogul, M. R. Kaçal, H. Polat, K. Dilsiz, O. Agar, *Advanced Composites* (Ed. S.J. Ikhmayies), Springer, Switzerland **2023**, Ch. 6.
[36] V. Harish, N. Nagaiah, T. N. Prabhu, K. T. Varughese, *J. Appl. Polym. Sci.* **2009**, *112*, 1503.
[37] M. Ferry, G. Roma, F. Cochin, S. Esnouf, V. Dauvois, F. Nizeyimana, B. Gervais, Y. Ngono-Ravache, *Polymers in the nuclear power industry*, (Ed. R. Konings), Elsevier, Oxford **2020**, Ch. 3.16.
[38] L. Gerward, N. Guilbert, K. Jensen, H. Levring, *Radiat. Phys. Chem.* **2004**, *71*, 653.
[39] S. Agostinelli, J. Allison, K. Amako, J. Apostolakis, H. Araujo, P. Arce, M. Asai, D. Axen, S. Banerjee, G. Barrand, F. Behner, L. Bellagamba, J. Boudreau, L. Broglia, A. Brunengo, H. Burkhardt, S. Chauvie, J. Chuma, R. Chytracek, G. Cooperman, *Nucl. Instrum. Methods Phys. Res. A* **2003**, *506*, 250.
[40] T. T. Böhlen, F. Cerutti, M. P. W. Chin, A. Fassò, A. Ferrari, P. G. Ortega, A. Mairani, P. R. Sala, G. Smirnov, V. Vlachoudis, *Nucl. Data Sheets* **2014**, *120*, 211.
[41] M. I. Sayyed, F. Akman, M. R. Kaçal, *Radiochim. Acta* **2019**, *107*, 339.
[42] H. Polat, C. Özel, *Radiat. Phys. Chem.* **2024**, *223*, 111963.
[43] H. Polat, C. Özel, *Mater. Chem. Phys.* **2024**, *323*, 129596.
[44] M. R. Kaçal, H. A. Karataş, F. Akman, *J. Radiol. Oncol.* **2017**, *1*, 60.
[45] F. C. Hila, A. Asuncion-Astronomo, C. A. M. Dingle, J. F. M. Jecong, A. M. V. Javier-Hila, M. B. Z. Gili, C. V. Balderas, G. E. P. Lopez, N. R. D. Guillermo, A. V. Amorsolo Jr., *Radiat. Phys. Chem.* **2021**, *182*, 109331.
[46] D. E. Cullen, *A Survey of Photon Cross Section Data for Use in EPICS2017*, IAEA (Int. Atomic Energy Agency), Vienna, Austria **2018**.
[47] D. A. Brown, M. B. Chadwick, R. Capote, A. C. Kahler, A. Trkov, M. W. Herman, A. A. Songozni, Y. Danon, A. D. Carlson, M. Dunn, D. L. Smith, G. M. Hale, Y. Zhu, *Nucl. Data Sheets* **2018**, *148*, 1.
[48] F. Akman, H. Oğul, M. F. Turhan, C. Ş. Ağrılı, *Radiat. Phys. Chem.* **2014**, *215*, 111376.
[49] ANSI/ANS-6.4.3, *Gamma Ray Attenuation Coefficient and Buildup Factors for Engineering Materials*, American Nuclear Society, La Grange Park, IL USA **1991**.
[50] M. F. Turhan, F. Akman, M. R. Kaçal, H. Polat, İ. Demirkol, *Appl. Radiat. Isot.* **2023**, *191*, 110568.
[51] M. F. Turhan, *Appl. Radiat. Isot.* **2021**, *177*, 109920.
[52] J. H. Hubbell, S. M. Seltzer, *Tables of x-ray mass attenuation coefficients and mass energy-absorption coefficients 1 keV to 20 meV for elements z = 1 to 92 and 48 additional substances of dosimetric interest*, National Inst. of Standards and Technology-PL, Gaithersburg, MD, USA **1995**.
[53] A. M. El-Khayatt, *Ann. Nucl. Energy* **2010**, *37*, 218.

